PHYSICAL REVIEW D **95,** 043506 (2017)

Resurrection of large lepton number asymmetries from neutrino flavor oscillations

Gabriela Barenboim,[1,*] William H. Kinney,[2,†] and Wan-Il Park[1,‡]

[1]*Departament de Física Teòrica and IFIC, Universitat de València-CSIC, E-46100 Burjassot, Spain*
[2]*Department of Physics, University at Buffalo, 239 Fronczak Hall, Buffalo, New York 14260-1500, USA*

(Received 13 September 2016; published 8 February 2017)

We numerically solve the evolution equations of neutrino three-flavor density matrices, and show that, even if neutrino oscillations mix neutrino flavors, large lepton number asymmetries are still allowed in certain limits by big bang nucleosynthesis.

DOI: 10.1103/PhysRevD.95.043506

I. INTRODUCTION

Despite the fact that the baryon number asymmetry of the Universe is constrained to be $B \sim 10^{-10}$ by big bang nucleosynthesis (BBN) [1] and observations of the cosmic microwave background (CMB) [2], the Universe is allowed to have a large lepton number asymmetry (L defined similarly to B but for leptons) as long as such an asymmetry is associated with neutral particles. In particular, a large asymmetry of neutrinos [e.g. $L \gtrsim \mathcal{O}(1)$] is quite attractive in view of its impacts on cosmology (for example, as a solution to the problem of topological defects via a symmetry nonrestoration [3,4], generation of B from L via sphaleron [5], and/or as a contribution to the extra relativistic species $\Delta N_{\rm eff}$ which may lead to a better fit to cosmological data). Even if the total lepton number vanishes, $L = 0$, the asymmetry L_α (for a neutrino flavor ν_α) could be large enough to have an impact on the generation of B [6] and $\Delta N_{\rm eff}$.

The main constraints on large neutrino asymmetries come from BBN (especially the abundance of ^{4}He) [7,8] and $\Delta N_{\rm eff}$, which is constrained by both BBN and CMB observations [2]. In particular, BBN strongly constrains the asymmetry of electron neutrinos such that the degeneracy parameter ($\xi_\alpha \equiv \mu_\alpha/T$, with μ_α being the chemical potential of ν_α and T the temperature) is constrained as [9]

$$-0.018 \le \xi_e \le 0.008 \Rightarrow -4.5 \lesssim 10^3 L_e \lesssim 2.0, \quad (1)$$

while recent Planck satellite data of CMB observations constrain $\Delta N_{\rm eff} \lesssim 0.36$ at 95% C.L. (Planck, TT, TE, EE + lowP + BAO) [2] which conventionally translates to

$$|\xi_{\mu,\tau}| \lesssim 0.89 \Rightarrow |L_{\mu,\tau}| \lesssim 0.24, \quad (2)$$

where $L_\alpha \equiv (n_\alpha - n_{\bar\alpha})/n_\gamma$ with $n_\alpha/n_{\bar\alpha}$ and n_γ being the number density of $\nu_\alpha/\bar\nu_\alpha$ and photons, respectively.

*Gabriela.Barenboim@uv.es
†whkinney@buffalo.edu
‡Wanil.Park@uv.es

Meanwhile, there has been a series of works showing that neutrino oscillations in the early universe mix three neutrinos such that any asymmetry $L_{\mu,\tau}$ which is established well before BBN is converted significantly to L_e [9–15] (see also [16]). As a result, although in Ref. [17] it was shown that sizable asymmetries of $\nu_{\mu,\tau}$ leading to large $\Delta N_{\rm eff}$ of $\mathcal{O}(0.1–1)$ are possible, this was the case only for $\theta_{13} = 0$. Later, Refs. [9,14] showed that for a nonzero θ_{13}, as measured by experimental observations, BBN requires $|L_{\mu,\tau}| \lesssim 0.1$ which translates to $\Delta N_{\rm eff} \lesssim 0.07$.

However, in these numerical simulations, the quantum kinetic equations of neutrino/antineutrino density matrices were solved using a scheme such that the mixed three-flavor neutrino system was handled as successive effective two-flavor systems (ν_μ-ν_τ and ν_e-$\nu_{\mu,\tau}$) before and after ν_μ-ν_τ equalization, as can be seen by the fact that the ν_μ-ν_τ degeneracy once established is never lifted [18], which is not consistent with the three mixing angles being nonzero, as will be discussed below. For the evolution up to the point of ν_μ-ν_τ equilibrium, the two-flavor description is enough since ν_e participates in the oscillations only afterwards. However, once ν_e is involved, the evolution of the mixed three-flavor system becomes quite complicated, and the ν_μ-ν_τ equalization may not be maintained anymore. In addition, the choice of neutrino mixing parameters has a significant impact on the final asymmetry of each flavor after the mixing and oscillation effects settle the system to an equilibrium state. More importantly, the total asymmetry L does not need to be small as long as its contribution to B is suppressed by symmetry nonrestoration [22]. In this regard, it is worthwhile to reexamine the impact of *three-flavor oscillations* of neutrinos on the BBN bound of the lepton number asymmetries with all the mixing angles different from zero as experiments indicate.

In this paper, we argue that the effective two-flavor description of the mixed three-flavor neutrino system does not necessarily capture the real physics of neutrino oscillations in the early universe. We demonstrate our argument by presenting the numerical solution to the three-flavor evolution equations, which is different from the results in earlier work based on a two-flavor effective description. We also show that BBN still allows large asymmetries which can lead to $\Delta N_{\rm eff} \sim \mathcal{O}(1)$.

II. TWO- OR THREE-FLAVOR DESCRIPTION?

The masses and mixing parameters of neutrino oscillations are now measured to be [1,23]

$$\Delta m^2_{21} = 7.53^{+0.18}_{-0.18} \times 10^{-5}\ \mathrm{eV}^2 \tag{3}$$

$$\Delta m^2_{31} \simeq \Delta m^2_{32} = 2.67 \pm 0.12 \times 10^{-3}\ \mathrm{eV}^2 \tag{4}$$

and

$$\sin^2 2\theta_{12} = 0.846 \pm 0.021 \tag{5}$$

$$\sin^2 2\theta_{13} = 0.093 \pm 0.008 \tag{6}$$

$$\sin^2 \theta_{23} = 0.40^{+0.03}_{-0.02} (0.63^{+0.02}_{-0.03}), \tag{7}$$

where θ_{ij} are the mixing angles in the Pontecorvo-Maki-Nakagawa-Sakata (PMNS) mixing matrix [24,25] whose CP-violating phase is set zero here. In the early universe, the oscillations of neutrino flavors can be described by the evolutions of neutrino/antineutrino density matrices. For a mode of momentum p, the density matrices in the flavor basis of three active neutrinos $(\nu_e, \nu_\mu, \nu_\tau)$ can be expressed in terms of polarization vectors $\mathbf{P}/\overline{\mathbf{P}}$ and Gell-Mann matrices $\lambda_i (i = 1\text{–}8)$ as

$$\rho_p = \frac{1}{3} \sum_{i=0}^{8} P_i \lambda_i, \qquad \overline{\rho}_p = \frac{1}{3} \sum_{i=0}^{8} \overline{P}_i \lambda_i, \tag{8}$$

where λ_0 is the 3×3 identity matrix. Then, the evolution equations of ρ_p and $\overline{\rho}_p$ are given by [26,27] (see also [28])

$$i \frac{d\rho_p}{dt} = [\Omega + \sqrt{2} G_F (\rho - \overline{\rho}), \rho_p] + C[\rho_p] \tag{9}$$

$$i \frac{d\overline{\rho}_p}{dt} = [-\Omega + \sqrt{2} G_F (\rho - \overline{\rho}), \rho_p] + C[\overline{\rho}_p]. \tag{10}$$

In the above equations,

$$\Omega = \frac{M^2}{2p} - \frac{8\sqrt{2} G_F p E_\ell}{3 m_W^2}, \tag{11}$$

where M^2 is the mass-square matrix of neutrinos in the flavor basis, G_F the Fermi constant, m_W the mass of the W-boson, $E_\ell = \mathrm{diag}(E_{ee} + E_{\mu\mu}, E_{\mu\mu}, 0)$ the energy density of charged leptons, $\rho = (1/2\pi^2) \int_0^\infty \rho_p p^2 dp$ (and similarly for $\overline{\rho}$), and $C[\cdots]$ is the collision term.

Practically, we numerically solve the equations of motion (EOMs) of P_i and $\overline{P}_i$ derived from Eqs. (9) and (10). Those equations are mixed in a complicated way, and it is nontrivial to get an insight of what may happen unless a numerical integration is performed. It is also difficult to see if the maintenance of ν_μ-ν_τ equalization in an effective two-flavor description taken in earlier works still is valid in this case. However, it is instructive to note that, when one of the mixing angles is set zero with $\theta_{23} = \pi/4$, the mass-square matrix M^2 has a special pattern (for example, if $\theta_{13} = 0$, then $M^2_{12} = -M^2_{13}$ and $M^2_{22} = M^2_{33}$). In this case, ignoring self-interaction terms, which barely affect our results, and the subdominant collision terms in Eqs. (9) and (10), one can see that some pairs of $P_i^\pm$ s (for example, P_1^--P_4^- and P_2^+-P_5^+ where $P_i^\pm \equiv P_i \pm \overline{P}_i$) are likely to be driven in exactly the opposite way (see the Appendix). As a result, it becomes possible to have $P_3^- - \sqrt{3} P_8^- = 0$ and $d(P_3^- - \sqrt{3} P_8^-)/dt = 0$ simultaneously, and this implies that, once ν_μ-ν_τ equalization is achieved, it is likely to be maintained even if another nonzero mixing becomes active. This is the case in which the two-flavor description can be applicable. However, if all the mixing angles are nonzero as the accumulated neutrino oscillation data indicate, or $\theta_{23} \neq \pi/4$ even if $\theta_{12} = 0$ or $\theta_{13} = 0$, the special pattern of the square-mass matrix disappears, and there is no reason to expect ν_μ-ν_τ equalization to be maintained once the second and/or third mixing get involved. Hence, we can expect that the two-flavor description may be applicable only to that limited case, which does not apply in view of the current observational data in neutrino oscillation experiments. In the next section, we will show that this is in fact the case.

III. RESULTS OF THREE-FLAVOR NUMERICAL INTEGRATION

In our numerical analysis, M^2 was taken to correspond to a normal hierarchy of neutrino masses. Also, since a precise treatment of collision terms has only a minor effect in the scope of this paper (see for example [19]), we take for simplicity $C[\rho_p] = -i D_{\alpha\beta} [\rho_p]_{\alpha\beta}$ for $\alpha \neq \beta$ only, and similarly for $C[\overline{\rho}_p]$ [11]. The initial condition for the simulations was set as

$$\rho_p = f(y, 0)^{-1} \mathrm{diag}(f(y, \xi_e), f(y, \xi_\mu), f(y, \xi_\tau)), \tag{12}$$

and similarly for $\overline{\rho}_p$ but with $\xi_\alpha \to -\xi_\alpha$, where $f(y, \xi_\alpha) = (e^{y - \xi_\alpha} + 1)^{-1}$ is the occupation number of ν_α for a mode $y \equiv p/T$.

In the presence of charged lepton backgrounds and/or collisional dampings, the dynamics of the occupation number of a mode is not oscillationlike, but transitionlike. In this case, the dynamics of flavor asymmetries (as a mode-integrated collective behavior) can be mimicked by a typical mode (i.e., corresponding to the averaged momentum or close to it) even without the self-interaction term [i.e., the term proportional to $\rho - \overline{\rho}$ in Eq. (9) or (10)], modulo an overall normalization [13]. We take this single

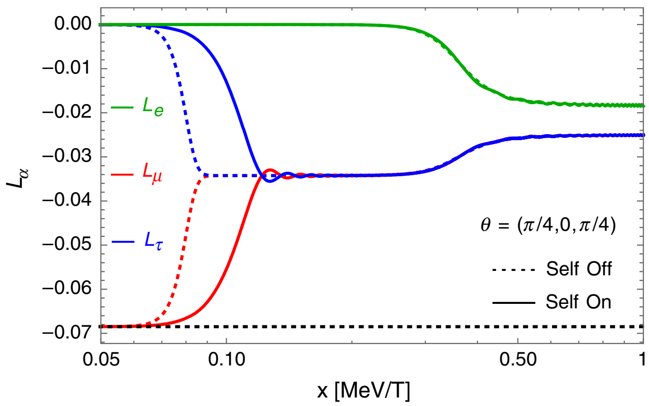

FIG. 1. Evolutions of L_α for $\theta = (\theta_{12}, \theta_{13}, \theta_{23})$ and $(\xi_e, \xi_\mu, \xi_\tau) = (0, -0.1, 0)$ with self-interaction switched on/off (solid/dotted lines). The green/red/blue line is for $L_e/L_\mu/L_\tau$. The black dotted line is the total asymmetry.

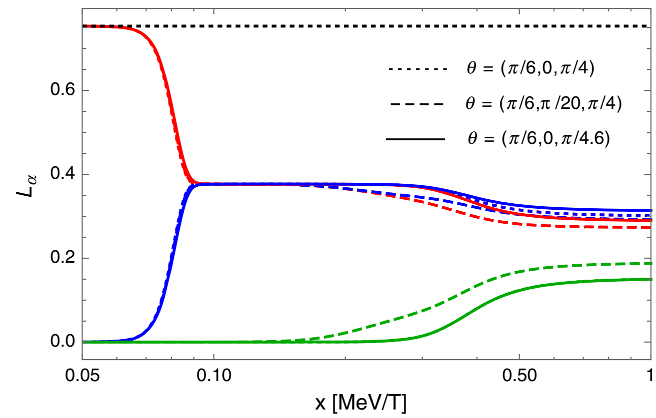

FIG. 2. Evolutions of L_α for $\theta = (\theta_{12}, \theta_{13}, \theta_{23})$ and $(\xi_e, \xi_\mu, \xi_\tau) = (0, 1, 0)$ with self-interaction switched on. The color scheme is the same as Fig. 1.

mode approach with $y = 3.15$ which is nearly the same as the mode of average momentum, but in order not to miss the specific phenomena caused by self-interaction (e.g., blocking of transition [11]), we keep the self-interaction term in a way that ρ^- ($\equiv \rho - \bar{\rho}$) is replaced by ρ_p^- ($\equiv \rho_p - \bar{\rho}_p$), normalized initially to match ρ^-. In order to see the result in terms of the lepton number asymmetries, the initial occupation numbers of our reference mode were normalized to match the initial lepton number asymmetries accounting all modes.

The validity of our approach was checked by reproducing some results in earlier works, for example, as shown in Fig. 1 (see Fig. 5 of Ref. [11] for comparison). The figure shows that the main features of the evolution of L_α governed by Eqs. (9) and (10) are captured by our simplified approach, proving the validity of our approach. The minor difference of the amplitude of synchronized oscillation (which depend on $|\eta_\alpha|$ or ξ_α) may be the difference between effective two-flavor description and three-flavor full description. If the initial asymmetries are large enough and are not forced to obey a specific pattern (e.g., equal and opposite), the evolution of the asymmetries appears to be essentially independent of the self-interaction term. This implies that for aligned initial asymmetries, when the self-interaction is large enough, $\mathbf{P}^+$ hardly deviates from the direction of $\mathbf{I}^- \equiv \sqrt{2} G_F \int \mathbf{P}^- p^2 dp / (2\pi^2)$ (or simply $\mathbf{P}^-$ in our simplified simulation).

As our first new result, Fig. 2 shows the evolution of L_α with different sets of mixing angles. The self-interaction term did not make any meaningful change in this case, as expected. As shown in the figure, the first dynamics takes place due to $\theta_{23} \sim \pi/4$ which mixes ν_μ and ν_τ completely, leading to $L_\mu = L_\tau$ irrespective of the value of θ_{23} due to frequent collisions. At later time, collisions become inefficient. In this circumstance, if $\theta_{23} = \pi/4$ and $\theta_{13} = 0$ (dotted lines), this equalization is maintained even if nonzero θ_{12} gets involved later. Checking the dynamics of all components of polarization vectors, we found that the reason for such a behavior is exactly what is discussed in the previous section. The same behavior appears if θ_{12} is set zero instead of θ_{13}. On the other hand, if all the mixing angles are nonzero (dashed lines) or $\theta_{23} \neq \pi/4$ (solid lines), the equalization is broken, as the second dynamics appears due to another mixing. Therefore, we conclude that, for the neutrino mixing parameters measured so far, $L_\mu \neq L_\tau$ as a result of neutrino mixings.

Obviously, the final L_α depends on L. So, we now consider some initial values of L_α for $L = 0$ and $L \neq 0$ cases as shown in Figs. 3 and 4, respectively. In the case of Fig. 3, due to the equal and opposite asymmetries of ν_μ and ν_τ, neutrino self-interaction blocks the ν_μ-ν_τ mixing until the dynamics due to the nonzero θ_{13} becomes active. This phenomenon was observed already in an earlier work [11], but the subsequent synchronized oscillation was not clear in the result, in contrast to our case. The large synchronized oscillation seems to be due to the delayed mixing of ν_μ-ν_τ that is dominated by the vacuum contribution in Eq. (11). The final asymmetries depend on the mixing

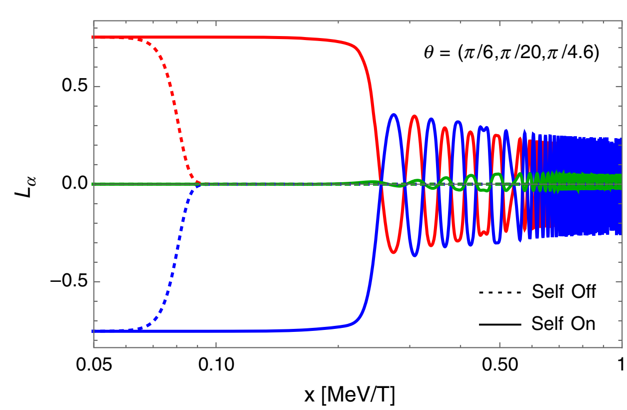

FIG. 3. Evolutions of L_α for $\theta = (\theta_{12}, \theta_{13}, \theta_{23})$ and $(\xi_e, \xi_\mu, \xi_\tau) = (0, 1, -1)$. The color scheme is the same as Fig. 1.

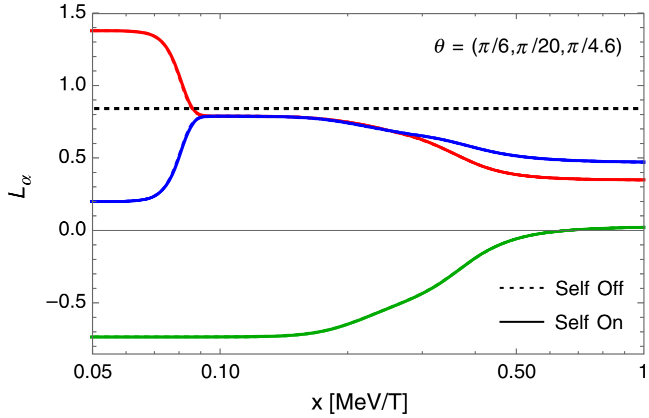

FIG. 4. Evolutions of L_α for $\theta = (\theta_{12}, \theta_{13}, \theta_{23})$ and $(\xi_e, \xi_\mu, \xi_\tau) = (-1.0, 1.6, 0.3)$. The color scheme is the same as Fig. 1. Dotted lines (the case of "Self Of") were overlapped by solid lines.

angles and configuration of $L_{\alpha,0}$. However, for $L = 0$, even if $L_{e,0} = 0$, the oscillation-averaged values turn out to be

$$|L_e| \sim |L_{\mu,\tau}| \lesssim 10^{-2} |L_{\mu,0}|, \tag{13}$$

where $L_{\alpha,0}$ is the initial asymmetry of ν_α, and $\xi_{\alpha,0} \lesssim 1$ was assumed. Hence, in this case we end up with the same conclusion as earlier works.

Contrary to the case of $L = 0$, if $L \neq 0$, one can take arbitrary initial values of L_α. This means that, as shown in Fig. 4, at the late time equilibrium it is possible to have small L_e but large $|L_{\mu,\tau}|$ which can result in $\Delta N_{\rm eff} \sim \mathcal{O}(1)$. Note that the net asymmetry L can be large enough to suppress the conversion of L to B by symmetry nonrestoration [29]. This is our main result.

Finally, in Fig. 5 we show the θ_{23}-dependence of L_α for $\theta_{23} = (\pi/3.4, \pi/4, \pi/4.6)$ which covers the favored values at NOνA data [23]. In the figure, one can see that for given nonzero values of $\theta_{12,13}$ the larger θ_{23} the smaller L_μ-L_τ

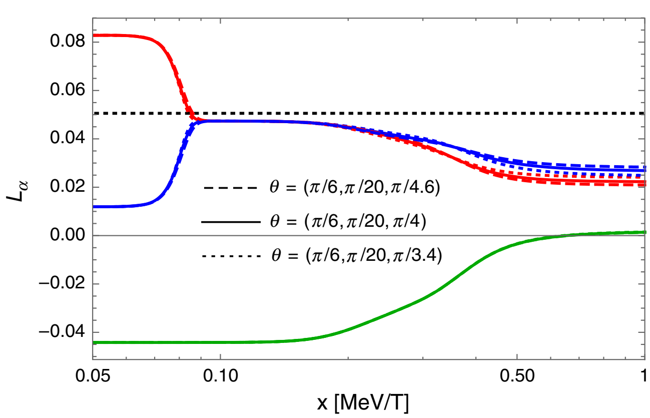

FIG. 5. Evolutions of L_α for $\theta = (\theta_{12}, \theta_{13}, \theta_{23})$ and $(\xi_e, \xi_\mu, \xi_\tau) = (-1.0, 1.6, 0.3)$ with self-interaction turned on. The color scheme is the same as Fig. 1.

separation, keeping the average of L_μ and L_τ barely changed (or L_e barely changed). This behavior is nontrivial, but one may get an idea from the evolution equations associated with L_α (see the Appendix): Ignoring self-interaction terms, for $\rho_p^\pm \equiv \rho_p \pm \bar{\rho}_p$ one finds

$$\left.\frac{d\rho_p^-}{dt}\right|_{ee} = \frac{2}{3}(\Omega_{12} P_2^+ + \Omega_{13} P_5^+) \tag{14}$$

$$\left.\frac{d\rho_p^-}{dt}\right|_{\mu\mu} = -\frac{2}{3}(\Omega_{12} P_2^+ - \Omega_{23} P_7^+) \tag{15}$$

$$\left.\frac{d\rho_p^-}{dt}\right|_{\tau\tau} = -\frac{2}{3}(\Omega_{13} P_5^+ + \Omega_{23} P_7^+), \tag{16}$$

where Ω_{ij} for $i \neq j$ can be approximated as

$$\Omega_{12} \approx \Delta m_{31}^2 c_{13} s_{13} s_{23} \tag{17}$$

$$\Omega_{13} \approx \Delta m_{31}^2 c_{13} s_{13} c_{23} \tag{18}$$

$$\Omega_{23} \approx \Delta m_{32}^2 c_{13}^2 c_{23} s_{23}. \tag{19}$$

It is not easy to see how P_2^+, P_5^+, and P_7^+ would depend on θ_{23}. However, from the property of the Pontecorvo-Maki-Nakagawa-Sakata (PMNS) matrix [24,25] describing neutrino mixings, it is clear that the evolution of $(\rho_p^-)_{ee}$ is invariant under the change of θ_{23}. This implies that the θ_{23}-dependence in the right-hand side of Eq. (14) is canceled out. Hence, from Eqs. (15)–(19) one finds that the evolutions of $(\rho_p^-)_{\mu\mu}$ and $(\rho_p^-)_{\tau\tau}$ should depend on θ_{23} in an equal and opposite way, but they are not symmetric with respect to $\theta_{23} = \pi/4$, as shown in Fig. 5. The impact of θ_{13} on L_α can be easily read off from Fig. 2, and it is straightforward to see that the larger θ_{12} the closer L_e and $L_{\mu,\tau}$.

IV. CONCLUSIONS

In this paper, we showed that, contrary to the widely held conventional expectation, lepton number asymmetries of neutrinos can be quite large while keeping the asymmetry of electron-neutrino small enough to satisfy the BBN bound. Large asymmetries of muon- and tau-neutrinos are expected to be constrained mainly by CMB through $\Delta N_{\rm eff}$ (extra neutrino species or "dark" radiation), but the asymmetries are better constrained in terms of neutrino mass eigenstates instead of flavor eigenstates [30].

In the literature, even if there were several works in which integrations of the full three-flavor evolution equations were considered in some contexts, an effective two-flavor description after the first transition between muon- and tau-neutrinos has been used by fixing the asymmetries of ν_μ and ν_τ equal as a kind of conventional method in the estimation of late time neutrino asymmetries in the presence of neutrino oscillations.

The neutrino asymmetries in this case were tightly constrained, leading to $\Delta N_{\rm eff} \lesssim 0.07$. However, such a setting is questionable in the presence of *three nonzero* mixing angles. In addition, neither BBN nor CMB data forbid a large nonzero total lepton number asymmetry. Motivated by these observations, we numerically integrated the quantum kinetic equations of the full three-flavor density matrices of neutrinos and antineutrinos, and found that the asymmetries of ν_μ and ν_τ after all the transitions are finished before BBN are actually different, and can be large enough to result in $\Delta N_{\rm eff} \sim \mathcal{O}(0.1\text{–}1)$ which is an order of magnitude larger than the one in earlier literature and may lead to a better fit to cosmological data [30].

For large arbitrary initial lepton number asymmetries well before BBN, the stringent BBN bound on the asymmetry of electron neutrinos appears to require a fine-tuning of the initial condition. However, such a tuning is certainly allowed by data, and could well be explained by some physics beyond the standard model.

ACKNOWLEDGMENTS

The authors are grateful to Sergio Pastor for his helpful comments. G. B. and W. I. P. also acknowledge support from the Ministerio de Educación y Ciencia (MEC) and Fondo Europeo de Desarrollo Regional (FEDER) (EC) Grants No. SEV-2014-0398 and No. FPA2014-54459 and the Generalitat Valenciana under Grant No. PROMETEOII/2013/017. This project has received funding from the European Unions Horizon 2020 research and innovation program under the Marie Sklodowska-Curie grant Elusives ITN Agreement No. 674896 and InvisiblesPlus RISE (Research and Innovation Staff Exchange), Agreement No. 690575. W. H. K. is supported by the U.S. National Science Foundation under Grant No. NSF-PHY-1417317. W. H. K. thanks the University of Valencia, where part of this work was completed, for hospitality and support.

APPENDIX POLARIZATION VECTOR EQUATIONS OF MOTIONS

From Eqs. (9) and (10), when the self-interaction terms are ignored, the equations of motion (EOMs) of P_i and $\overline{P}_i$ are derived as follows:

$$\dot{P}_0 = 0 \tag{A1}$$

$$\dot{P}_1 = -D_{12}P_1 - (\Omega_{11} - \Omega_{22})P_2 + \Omega_{23}P_5 + \Omega_{13}P_7 \tag{A2}$$

$$\dot{P}_2 = (\Omega_{11} - \Omega_{22})P_1 - D_{12}P_2 - 2\Omega_{12}P_3 - \Omega_{23}P_4 + \Omega_{13}P_6 \tag{A3}$$

$$\dot{P}_3 = 2\Omega_{12}P_2 + \Omega_{13}P_5 - \Omega_{23}P_7 \tag{A4}$$

$$\dot{P}_4 = \Omega_{23}P_2 - D_{13}P_4 - (\Omega_{11} - \Omega_{33})P_5 - \Omega_{12}P_7 \tag{A5}$$

$$\dot{P}_5 = -\Omega_{23}P_1 + (\Omega_{11} - \Omega_{33})P_4 - D_{13}P_5 + \Omega_{12}P_6 - \Omega_{13}(P_3 + \sqrt{3}P_8) \tag{A6}$$

$$\dot{P}_6 = -\Omega_{13}P_2 - \Omega_{12}P_5 - D_{23}P_6 - (\Omega_{22} - \Omega_{33})P_7 \tag{A7}$$

$$\dot{P}_7 = -\Omega_{13}P_1 + \Omega_{12}P_4 + (\Omega_{22} - \Omega_{33})P_6 - D_{23}P_7 + \Omega_{23}(P_3 - \sqrt{3}P_8) \tag{A8}$$

$$\dot{P}_8 = \sqrt{3}(\Omega_{13}P_5 + \Omega_{23}P_7). \tag{A9}$$

EOMs of $\overline{P}_i$ are obtained by taking $\Omega_{ij} \to -\Omega_{ij}$ and $P_i \to \overline{P}_i$ in the above equations. Hence, for $P_i^\pm \equiv P_i \pm \overline{P}_i$ one finds

$$\dot{P}_0^\mp = 0 \tag{A10}$$

$$\dot{P}_1^\mp = -D_{12}P_1^\mp - (\Omega_{11} - \Omega_{22})P_2^\pm + \Omega_{23}P_5^\pm + \Omega_{13}P_7^\pm \tag{A11}$$

$$\dot{P}_2^\mp = (\Omega_{11} - \Omega_{22})P_1^\pm - D_{12}P_2^\mp - 2\Omega_{12}P_3^\pm - \Omega_{23}P_4^\pm + \Omega_{13}P_6^\pm \tag{A12}$$

$$\dot{P}_3^\mp = 2\Omega_{12}P_2^\pm + \Omega_{13}P_5^\pm - \Omega_{23}P_7^\pm \tag{A13}$$

$$\dot{P}_4^\mp = \Omega_{23}P_2^\pm - D_{13}P_4^\mp - (\Omega_{11} - \Omega_{33})P_5^\pm - \Omega_{12}P_7^\pm \tag{A14}$$

$$\dot{P}_5^\mp = -\Omega_{23}P_1^\pm + (\Omega_{11} - \Omega_{33})P_4^\pm - D_{13}P_5^\mp + \Omega_{12}P_6^\pm - \Omega_{13}(P_3^\pm + \sqrt{3}P_8^\pm) \tag{A15}$$

$$\dot{P}_6^\mp = -\Omega_{13}P_2^\pm - \Omega_{12}P_5^\pm - D_{23}P_6^\mp - (\Omega_{22} - \Omega_{33})P_7^\pm \tag{A16}$$

$$\dot{P}_7^\mp = -\Omega_{13}P_1^\pm + \Omega_{12}P_4^\pm + (\Omega_{22} - \Omega_{33})P_6^\pm - D_{23}P_7^\mp + \Omega_{23}(P_3^\pm - \sqrt{3}P_8^\pm) \tag{A17}$$

$$\dot{P}_8^\mp = \sqrt{3}(\Omega_{13}P_5^\pm + \Omega_{23}P_7^\pm). \tag{A18}$$

[1] K. A. Olive *et al.* (Particle Data Group Collaboration), Review of particle physics, Chin. Phys. C **38**, 090001 (2014).

[2] P. A. R. Ade *et al.* (Planck Collaboration), Planck 2015 results. XIII. Cosmological parameters, Astron. Astrophys. **594**, A13 (2016).

[3] A. Riotto and G. Senjanovic, Supersymmetry and Broken Symmetries at High Temperature, Phys. Rev. Lett. **79**, 349 (1997).

[4] B. Bajc, A. Riotto, and G. Senjanovic, Large Lepton Number of the Universe and the Fate of Topological Defects, Phys. Rev. Lett. **81**, 1355 (1998).

[5] J. Liu and G. Segre, Baryon asymmetry of the universe and large lepton asymmetries, Phys. Lett. B **338**, 259 (1994).

[6] J. March-Russell, H. Murayama, and A. Riotto, The small observed baryon asymmetry from a large lepton asymmetry, J. High Energy Phys. 11 (1999) 015.

[7] F. Iocco, G. Mangano, G. Miele, O. Pisanti, and P. D. Serpico, Primordial nucleosynthesis: From precision cosmology to fundamental physics, Phys. Rep. **472**, 1 (2009).

[8] R. H. Cyburt, B. D. Fields, K. A. Olive, and T. H. Yeh, Big bang nucleosynthesis: 2015, Rev. Mod. Phys. **88**, 015004 (2016).

[9] G. Mangano, G. Miele, S. Pastor, O. Pisanti, and S. Sarikas, Updated BBN bounds on the cosmological lepton asymmetry for nonzero θ_{13}, Phys. Lett. B **708**, 1 (2012).

[10] C. Lunardini and A. Y. Smirnov, High-energy neutrino conversion and the lepton asymmetry in the universe, Phys. Rev. D **64**, 073006 (2001).

[11] A. D. Dolgov, S. H. Hansen, S. Pastor, S. T. Petcov, G. G. Raffelt, and D. V. Semikoz, Cosmological bounds on neutrino degeneracy improved by flavor oscillations, Nucl. Phys. **B632**, 363 (2002).

[12] Y. Y. Y. Wong, Analytical treatment of neutrino asymmetry equilibration from flavor oscillations in the early universe, Phys. Rev. D **66**, 025015 (2002).

[13] K. N. Abazajian, J. F. Beacom, and N. F. Bell, Stringent constraints on cosmological neutrino antineutrino asymmetries from synchronized flavor transformation, Phys. Rev. D **66**, 013008 (2002).

[14] G. Mangano, G. Miele, S. Pastor, O. Pisanti, and S. Sarikas, Constraining the cosmic radiation density due to lepton number with big bang nucleosynthesis, J. Cosmol. Astropart. Phys. 03 (2011) 035.

[15] E. Castorina, U. Franca, M. Lattanzi, J. Lesgourgues, G. Mangano, A. Melchiorri, and S. Pastor, Cosmological lepton asymmetry with a nonzero mixing angle θ_{13}, Phys. Rev. D **86**, 023517 (2012).

[16] L. Johns, M. Mina, V. Cirigliano, M. W. Paris, and G. M. Fuller, Neutrino flavor transformation in the lepton-asymmetric universe, Phys. Rev. D **94**, 083505 (2016).

[17] S. Pastor, T. Pinto, and G. G. Raffelt, Relic Density of Neutrinos with Primordial Asymmetries, Phys. Rev. Lett. **102**, 241302 (2009).

[18] It should be noted that, even if in Ref. [11] the full evolution equations including the three-flavors were solved, since then an effective two-flavor description has been the standard lore in the analysis of neutrino lepton number asymmetries under neutrino oscillations. There have been nevertheless several works with full three-flavor evolutions and a clear distinction between ν_μ and ν_τ (see for example [19–21]) but in a different context (involving either zero or rather small total asymmetries).

[19] P. F. de Salas and S. Pastor, Relic neutrino decoupling with flavour oscillations revisited, J. Cosmol. Astropart. Phys. 07 (2016) 051.

[20] G. Mangano, G. Miele, S. Pastor, T. Pinto, O. Pisanti, and P. D. Serpico, Relic neutrino decoupling including flavor oscillations, Nucl. Phys. **B729**, 221 (2005).

[21] J. Gava and C. Volpe, *CP* violation effects on the neutrino degeneracy parameters in the early Universe, Nucl. Phys. **B837**, 50 (2010).

[22] The required lepton number asymmetry for a large enough symmetry breaking is much larger than the asymmetry allowed by CMB. Therefore, there should be some amount of entropy production below electroweak scale temperature in order to reduce the initial large asymmetry to a safe level.

[23] https://www-nova.fnal.gov/.

[24] Z. Maki, M. Nakagawa., and S. Sakata, Remarks on the unified model of elementary particles, Prog. Theor. Phys. **28**, 870 (1962).

[25] B. Pontecorvo, Mesonium and anti-mesonium, Zh. Eksp. Teor. Fiz. **33**, 549 (1957) [Sov. Phys. JETP **6**, 429 (1957)].

[26] G. Sigl and G. Raffelt, General kinetic description of relativistic mixed neutrinos, Nucl. Phys. **B406**, 423 (1993).

[27] J. T. Pantaleone, Neutrino oscillations at high densities, Phys. Lett. B **287**, 128 (1992).

[28] D. N. Blaschke and V. Cirigliano, Neutrino Quantum kinetic equations: The collision term, Phys. Rev. D **94**, 033009 (2016).

[29] B. Bajc and G. Senjanovic, Large lepton number and high temperature symmetry breaking in MSSM, Phys. Lett. B **472**, 373 (2000).

[30] G. Barenboim, W. H. Kinney, and W. I. Park, Flavor versus mass eigenstates in neutrino asymmetries: implications for cosmology, arXiv:1609.03200.